

A joint segmentation and reconstruction algorithm for 3D Bayesian Computed Tomography using Gaus-Markov-Potts Prior Model

Camille Chapdelaine, Ali Mohammad-Djafari, Nicolas Gac, Estelle
Parra-Denis

► **To cite this version:**

Camille Chapdelaine, Ali Mohammad-Djafari, Nicolas Gac, Estelle Parra-Denis. A joint segmentation and reconstruction algorithm for 3D Bayesian Computed Tomography using Gaus-Markov-Potts Prior Model. The 42nd IEEE International Conference on Acoustics, Speech and Signal Processing (ICASSP 2017), Mar 2017, New Orleans, United States. hal-01588443

HAL Id: hal-01588443

<https://hal.archives-ouvertes.fr/hal-01588443>

Submitted on 15 Sep 2017

HAL is a multi-disciplinary open access archive for the deposit and dissemination of scientific research documents, whether they are published or not. The documents may come from teaching and research institutions in France or abroad, or from public or private research centers.

L'archive ouverte pluridisciplinaire **HAL**, est destinée au dépôt et à la diffusion de documents scientifiques de niveau recherche, publiés ou non, émanant des établissements d'enseignement et de recherche français ou étrangers, des laboratoires publics ou privés.

A JOINT SEGMENTATION AND RECONSTRUCTION ALGORITHM FOR 3D BAYESIAN COMPUTED TOMOGRAPHY USING GAUSS-MARKOV-POTTS PRIOR MODEL

Camille Chapdelaine^{1,2}, Advisors : Ali Mohammad-Djafari¹, Nicolas Gac¹, Estelle Parra²

¹ Laboratoire des signaux et systèmes, CNRS, Centralesupélec-Univ Paris Saclay, Gif-sur-Yvette, France
²SAFRAN SA, Safran Tech, Pôle Technologie du Signal et de l'Information, Magny-Les-Hameaux, France

ABSTRACT

Gauss-Markov-Potts models for images and its use in many image restoration, super-resolution and Computed Tomography (CT) have shown their effective use for Non Destructive Testing (NDT) applications. In this paper, we propose a 3D Gauss-Markov-Potts model for 3D CT for NDT applications. Thanks to this model, we are able to perform a joint reconstruction and segmentation of the object to control, which is very useful in industrial applications. First, we describe our prior models for each unknown of the problem. Then, we present results on simulated data and compare them to those of Total Variation (TV) minimization algorithm. Two quality indicators exploiting the segmentation are also proposed.

Index Terms— Gauss-Markov-Potts, 3D Computed Tomography, joint reconstruction and segmentation

1. INTRODUCTION

Computed tomography (CT) is a powerful imaging tool to see the interior of a three dimensional object and has a wide field of applications. In particular, in industry, the most used one is the so-called FDK algorithm [1] for cone-beam CT, which performs a filtered back-projection (FBP) algorithm. This algorithm is part of analytical reconstruction methods, based on the use of Radon transform [2]. There exist other analytical reconstruction methods [3] which use Fourier slice theorem but need to apply a filter in order to deal with a tricky interpolation in Fourier domain.

These analytical reconstruction methods suffer from artifacts due to approximations and give poor results with limited-angle projections. From this standpoint, algebraic reconstruction techniques (ART) and iterative methods have been provided for the last decades and consider a linearized discretization of Radon transform [2]. In order to account for the errors and to obtain a better reconstruction, most of these methods apply a regularization which enforces some priors on the object to reconstruct [4].

In our application, we aim at reconstructing an industrial part which is composed of several materials filling one or several compact and quite homogeneous regions. Gauss-Markov-Potts model has been successfully applied in microwave imaging [5] and image restoration [6]. In this paper, we present a 3D Gauss-Markov-Potts model for CT for non-destructive testing (NDT) in industry, based on the works done in [6]. A joint maximization a posteriori (JMAP) is also proposed, which *jointly* retrieves an estimation of the object to reconstruct and a segmentation of the reconstructed object in compact and well-distinguishable regions.

2. MODELS

The forward model is based on the discretization of Radon transform. Denoting by \mathbf{g} the data, by \mathbf{f} the object to reconstruct and by \mathbf{H} the projection operator, we write the forward projection model :

$$\mathbf{g} = \mathbf{H}\mathbf{f} + \boldsymbol{\epsilon} \quad (1)$$

Errors ϵ_i are modeled as zero-mean Gaussian with unknown variances $(v_{\epsilon_i})_i, \forall i$, which are modeled as following an Inverse Gamma distribution :

$$p(v_{\epsilon_i} | \alpha_{\epsilon_0}, \beta_{\epsilon_0}) = \mathcal{IG}(v_{\epsilon_i} | \alpha_{\epsilon_0}, \beta_{\epsilon_0}), \forall i \quad (2)$$

where α_{ϵ_0} et β_{ϵ_0} are fixed hyperparameters.

For the object, as said in introduction, we use a Gauss-Markov-Potts model. We define a hidden field \mathbf{z} that labels each voxel by the material it represents : for instance, $z_j = k$ if voxel j is part of material k . We assume that the number K of materials in the object is known. Then, homogeneity of each material is enforced by modeling that the gray values of the voxels of a same material k are distributed around a mean value m_k , with variance v_k

$$p(f_j | z_j = k, m_k, v_k) = \mathcal{N}(f_j | m_k, v_k) \text{ if } z_j = k. \quad (3)$$

The priors for the means and the variances of the classes are

$$p(m_k | m_0, v_0) = \mathcal{N}(m_k | m_0, v_0) \quad (4)$$

and

$$p(v_k | \alpha_0, \beta_0) = \mathcal{IG}(v_k | \alpha_0, \beta_0) \quad (5)$$

where m_0, v_0, α_0 and β_0 are fixed hyperparameters. To translate the compacity of each material, we assign a Markov-Potts prior model for the hidden field \mathbf{z} :

$$p(\mathbf{z} | \boldsymbol{\alpha}, \gamma_0) \propto \exp \left[\sum_j \left(\sum_{k=1}^K \alpha_k \delta(z_j - k) + \gamma_0 \sum_{i \in \mathcal{V}(j)} \delta(z_j - z_i) \right) \right] \quad (6)$$

Parameter γ_0 allows to control the compactness of the regions, as shown in figure 1. Here, γ_0 is tuned sufficiently large so the regions are compact. These prior models are very similar to the ones proposed in [6] for image restoration. The main difficulty here is that we deal with very huge 3D objects : this makes matrix \mathbf{H} unstorable in memory.

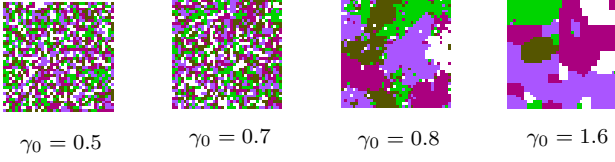


Fig. 1: Potts field z for different values of γ_0 , with $K = 5$ classes

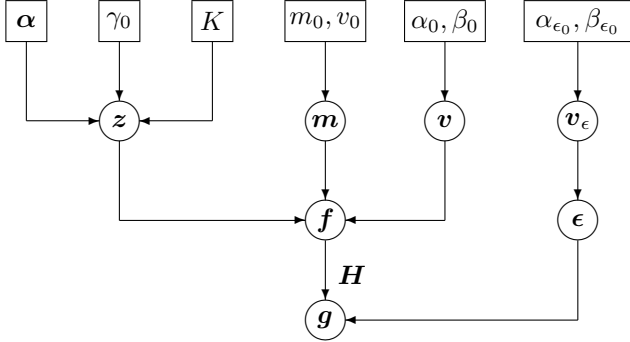


Fig. 2: Gauss-Markov-Potts hierarchical model

3. JOINT MAXIMIZATION AND RESULTS

Our hierarchical model is summarized in figure 2. We estimate the unknowns f , z , v_ϵ , m and v by maximizing the joint posterior distribution of the unknowns (JMAP) :

$$p(\mathbf{f}, \mathbf{z}, \mathbf{v}_\epsilon, \mathbf{m}, \mathbf{v} | \mathbf{g}; \mathcal{M}) \propto p(\mathbf{g} | \mathbf{f}, \mathbf{v}_\epsilon) p(\mathbf{f} | \mathbf{z}, \mathbf{m}, \mathbf{v}) p(\mathbf{v}_\epsilon | \alpha_{\epsilon_0}, \beta_{\epsilon_0}) p(\mathbf{z} | \alpha; \gamma_0) p(\mathbf{m} | m_0, v_0) p(\mathbf{v} | \alpha_0, \beta_0) \quad (7)$$

Equation (7) highlights the importance of our priors. Thanks to this expression, at iteration t of the algorithm, in order to estimate and update each unknown, we can successively maximize its posterior distribution given the other unknowns : this is an approximate maximization of the posterior distribution which makes possible to achieve joint reconstruction and segmentation of the controlled object.

The method is tested on 256^3 size Shepp-Logan 3D phantom, of which the middle slice is shown in figure (3a). The corresponding segmentation is shown in figure (3b): the number of materials is $K = 5$. 64 projections with 256^2 pixels are obtained from this phantom and are noisy with signal-to-noise ratio (SNR) equal to 20 db. Then, the algorithm is applied with $\gamma_0 = 3$ and the reconstruction and the segmentation, of which middle slices are shown in figures (3c) and (3d), are obtained. The core of the algorithm speedup is the parallelization on GPU of the projector H and backprojector H^T , which makes gradient descent in the object estimation step fast. For the reconstruction and segmentation in figures (3c) and (3d), we have achieved a total computation time about 10 minutes. The method is compared to Total Variation (TV) minimization algorithm, to which a posterior Potts segmentation is applied. The results for TV are shown in figures (3e) and (3f). TV reconstruction retrieves the bone better than our algorithm, but joint segmentation in figure (3d) retrieves the detail on the front while this is not the case in figure (3f), although it is retrieved in TV reconstruction. This emphasizes the great interest of joint reconstruction and segmentation, that is not cumulating errors from reconstruction and segmentation algorithms.

Moreover, we have used the segmentation to define two quality indicators designed so that the higher they are, the better the reconstruction is. The compactness indicator gives the

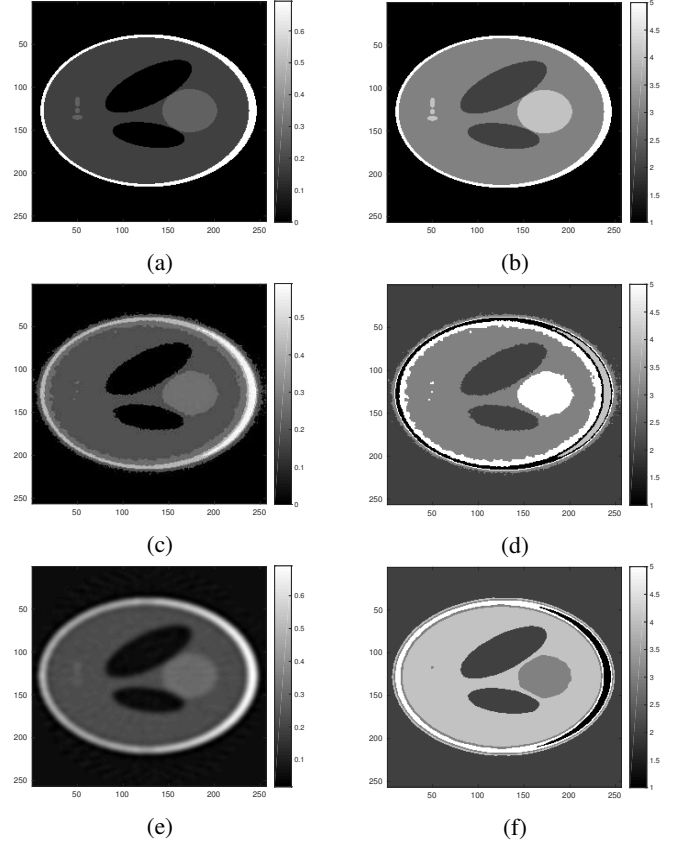


Fig. 3: Shepp-Logan 3D phantom (a) and its segmentation (b), obtained joint reconstruction (c) and segmentation (d) by our method, and obtained reconstruction by TV (e) and its posterior Potts segmentation (f) (middle slices)

average rate of voxels which are only surrounded by neighbours in the same class as them : it is 89.2% for our method reconstruction and 88.9% for TV. The distinguishability indicator measures how two voxels in different classes on the contours of the regions are distinguishable : it is 73.9% for our method reconstruction, and 72.8% for TV.

4. CONCLUSION AND PERSPECTIVES

In this paper, we have presented a comprehensive prior model to perform joint reconstruction and segmentation in 3D CT. This method has been shown to retrieve results comparable to TV. The two herein proposed quality indicators have made us able to see that joint segmentation is better than posterior segmentation. Future works will focus on full implementation on GPU and some variations in the prior model.

5. REFERENCES

- [1] L. Feldkamp, L. Davis, and J. Kress, "Practical cone-beam algorithm," *JOSA A*, vol. 1, no. 6, pp. 612–619, 1984.
- [2] K. T. Smith and F. Keinert, "Mathematical foundations of computed tomography," *Applied Optics*, vol. 24, no. 23, pp. 3950–3957, 1985.
- [3] J. I. Jackson, C. H. Meyer, D. G. Nishimura, and A. Macovski, "Selection of a convolution function for Fourier inversion using gridding [computerized tomography application]," *Medical Imaging, IEEE Transactions on*, vol. 10, no. 3, pp. 473–478, 1991.
- [4] A. Mohammad-Djafari and G. Demoment, "Maximum entropy image reconstruction in X-ray and diffraction tomography," *Medical Imaging, IEEE Transactions on*, vol. 7, no. 4, pp. 345–354, 1988.
- [5] O. Féron, B. Duchêne, and A. Mohammad-Djafari, "Microwave imaging of inhomogeneous objects made of a finite number of dielectric and conductive materials from experimental data," *Inverse Problems*, vol. 21, no. 6, p. S95, 2005.
- [6] H. Ayasso and A. Mohammad-Djafari, "Joint NDT image restoration and segmentation using Gauss-Markov-Potts prior models and variational bayesian computation," *Image Processing, IEEE Transactions on*, vol. 19, no. 9, pp. 2265–2277, 2010.